Effects of local moments on the magnetization of $HoBa_2Cu_3O_7$

O. B. Hyun and I. Hirabayashi
Superconductivity Research Laboratory, International Superconductivity Technology Center, 2-4-1 Mutsuno, Atsuta-Ku, Nagoya 456, Japan
(Received 3 February 1994)

The magnetic properties of $HoBa_2Cu_3O_7$ are investigated by taking account of the quantization of the induced Ho^{3+} moments to superconducting vortices. Based on the London model, we show that the induced moment decreases the penetration depth, and increases the equilibrium flux density by a factor of $(1+4\pi\chi)$, where χ is the susceptibility of the Ho^{3+} ions. Therefore, when the induced moment is greater than the Meissner diamagnetism, flux lines move into the specimen as temperature decreases and move out of it as temperature increases. This flux motion, together with flux pinning, causes different magnetization hysteresis, particularly in flux expulsion, from that of $YBa_2Cu_3O_7$.

I. INTRODUCTION

The superconductivity in the cuprates $RBa_2Cu_3O_7$ (RBCO), where R is the rare-earth elements with magnetic moments, is known to be independent of the local moments of R^{3+} ions or their magnetic order.[1,2] The interest of this study was the effects of the induced local moments on the flux density and magnetic properties for the cuprate superconductors. The local moment may produce a weak perturbation on both microscopic and macroscopic flux distribution and alter the magnetization. However, for the above cuprates, including the title compound, the role of the induced local moment of the R^{3+} ions has not been properly discussed. Some anomalies, such as the smallness of the measured moment of Ho^{3+} ions in $HoBa_2Cu_3O_7$ (HBCO) at low temperatures, were ascribed to insufficient flux penetration and strong crystal-field effects (CFE).[3-5]

In the course of studying the role of Ho^{3+} ions in the magnetization of HBCO, we observed a hysteretic flux expulsion at intermediate fields H ($H_{c1} \ll H \ll H_{c2}$). The hysteresis in the flux expulsion for type-II superconductors has been investigated theoretically[6] as well as experimentally for both low fields ($H \sim 10^2$ G or lower)[7] and intermediate fields ($H \sim 10^4$ G).[8] It has been known that $YBa_2Cu_3O_7$ (YBCO) shows hysteretic flux expulsion at low fields ($H \sim 10^2$ G), but negligible (or practically no) hysteresis in the flux expulsion for the field range $H \geq 10^4$ G.[8] However, the hysteresis in the flux expulsion of HBCO was observed at $H \sim 10^4$ G, and was greater the higher the H. Therefore, it became obvious that the flux expulsion behavior of HBCO could not be accounted by simple addition of local Ho^{3+} moments to the flux expulsion of YBCO. Since the critical-state model[9] adequately describes the magnetization as a function of field $M(H)$ (Ref. 10) and temperature $M(T)$ (Refs. 6–8, 11, and 12) for YBCO, it must be logical to expect that the model works equally well for HBCO. The critical-state model does account for the hysteretic flux expulsion of HBCO *if* the Ho^{3+} contribution in $M(T)$ were irreversible. This seeming irreversibility of the Ho^{3+} moment, which is because the induced moment is quantized to superconducting vortices, must be an example of electromagnetic interaction between the local moment and superconductivity in the cuprate superconductors.

For ferromagnetic (or antiferromagnetic) superconductors such as RRh_4B_4 or RMo_6S_8, however, the role of the local moments has been extensively investigated.[13-15] Maekawa, Tachiki, and Takahashi[13] discussed theoretically the quantization of superconducting vortices in the ferromagnetic superconductor $ErRh_4B_4$. They showed that the polarization of local spins induced by the supercurrent in a vortex is quantized along the magnetic field. As a result, the penetration depth λ is reduced by a factor of $\mu^{-1/2}$, where μ is the permeability of the spins. Description of the ferromagnetic superconductors includes consideration of various exchange interactions, pair breaking, nonlocality of the susceptibility and supercurrent, and so on. For instance, the magnetic isotherm for RRh_4B_4 was described by taking account of the electromagnetic interaction was well as the s-f exchange interaction between the conduction electron and local moments.[16] Therefore, one can predict the magnetic properties of RBCO by the same process. However, since the Néel temperature T_N [=0.14 K for HBCO (Ref. 17)] is too far from the measuring temperatures (>4 K), the exchange interactions, conduction-electron polarization, or any pair breaking may be safely ignored. In this sense, the above process would be ideal, but not practical for such simple systems as paramagnetic RBCO superconductors.

This study starts with the London model for nonmagnetic superconductors to describe the magnetization for RBCO. We treat the RBCO system as a linear paramagnetic medium with uniform susceptibility of Ho^{3+} ions with no exchange interactions between them. So, superconductivity is superposed on the medium without creating pair breaking. Based on the London model including the electromagnetic interaction between the local moments and superconductivity, we show that the local moments decrease the penetration depth, and increase the equilibrium flux density. The critical-state model is then applied to predict the flux expulsion, and the model pre-

diction is compared with the experimental data at intermediate fields for HBCO.

II. EQUILIBRIUM FLUX DENSITY IN A PARAMAGNETIC MEDIUM

Since HBCO is very much like YBCO, we can safely assume $\kappa \equiv \lambda/\xi \gg 1$, where κ is the Ginzburg-Landau parameter and ξ is the coherence length. Also, the induced moment of the magnetic ions is small, and linear with the local field in the measuring $T(\gg T_N)$ and $H(\leq 5$ T). Therefore, unlike the ferromagnetic superconductor case, we use the local electrodynamics for the susceptibility χ, the supercurrent $\mathbf{j}_S(\mathbf{r})$, and therefore, the London model $\mathbf{j}_S(\mathbf{r}) \propto \mathbf{A}(\mathbf{r})$, where $\mathbf{A}(\mathbf{r})$ is the vector potential at position $\mathbf{r}$. The local magnetic induction is $\mathbf{b}(\mathbf{r}) = \nabla \times \mathbf{A} = (1+4\pi\chi)\mathbf{h}(\mathbf{r}) = \mu \mathbf{h}(\mathbf{r})$ with $\mu = 1+4\pi\chi$. Here, $h(\mathbf{r})$ is the microscopic field due to j_S from $\nabla \times \mathbf{h} = (4\pi/c)\,\mathbf{j}_S$. In the surface region of thickness λ, the magnetic induction is enhanced by a factor of μ due to the induced moment as if the superconductor were in the larger field μH rather than the applied H. In the bulk region, because of b quantization, the induced moment is completely embedded in the vortex, and therefore contributes to the magnetization through the vortices. Consequently, the superconductor with paramagnetic ions may have more vortices than it would without them. Avoiding too much calculation, this is elaborated in terms of the free energy of a superconductor with magnetic ions. The free energy in the London model associated with the magnetic field for the superconducting HBCO system, which is a linear magnetic medium, may be written as[14]

$$F = \frac{1}{8\pi}\int [\mathbf{h}\cdot\mathbf{b} + \lambda_L^2 |\nabla \times \mathbf{h}|^2] d\mathbf{r}$$
$$= \left[\frac{1}{\mu}\right] \cdot \frac{1}{8\pi}\int [\mathbf{b}^2 + \lambda^2 |\nabla \times \mathbf{b}|^2] d\mathbf{r} \,. \quad (1)$$

Here, λ_L is the London penetration depth without local moments.[18] For an isolated vortex, F stands for the vortex line energy ϵ_1, and the integration is carried out over the plane normal to b except at the vortex core, ignoring the core contribution to the energy. Minimization of F with respect to b yields the London equation $\mathbf{b} + \lambda^2 \nabla \times \nabla \times \mathbf{b} = 0$ [or $\mathbf{b} + \lambda^2 \nabla \times \nabla \times \mathbf{b} = (\mathbf{b}/b)\phi_0 \delta(\mathbf{r})$ for a vortex including the core contribution], where $\lambda \equiv \lambda_L/\mu^{1/2}$ is the penetration depth in a magnetic medium.[13] Since χ is in the order of 10^{-2}, except at very low temperatures, λ is only slightly smaller than λ_L. However, the superconductor significantly reduces the penetration depth at very low temperatures near 1 K, due to the large susceptibility of the magnetic ions. ξ must be independent of χ in the absence of pair breaking. The decrease in λ simply makes a vortex slimmer. The flux density at a vortex core is $b(0) \approx (\phi_0/2\pi\lambda^2) K_0(\xi/\lambda) \approx \mu h_{\chi=0}(0)$, apart from the slowly varying K_0 term, where K_0 is the modified Bessel function of zero order and $h_{\chi=0}(0)$ is the field at the vortex core for $\chi = 0$ (no magnetic ions).[18,19] Thus, the vortex line energy $\epsilon_1 \approx (\phi_0/8\pi)[b(0)/\mu] \approx (\phi_0/8\pi) h_{\chi=0}(0)$ is approximately independent of χ, and so is $H_{c1} = (4\pi/\phi_0)\epsilon_1$. This is consistent with the fact that the magnetic ions have little effect without vortex penetration.

The increase of the Gibbs function density G_s associated with the magnetic field is

$$G_s = F - (1/4\pi)HB = \epsilon_1 (B/\phi_0) + \Sigma f_{ij} - (1/4\pi)HB \,,$$

where F is given by Eq. (1), B is the average flux density, and Σf_{ij} is the intervortex interaction. Since ϵ_1 is insensitive to χ, the χ dependence of G_s is in Σf_{ij}. A numerical estimation shows that Σf_{ij} varies as $\Sigma f_{ij}(\chi) \sim \mu^{-1} \Sigma f_{ij}(\chi = 0)$. The equilibrium B is obtained by minimizing G_s with respect to B, and is readily available in literature. For instance, repeating the process leading to Eq. (5-27) and Eq. (5-39) of Ref. 19, after considering the factor $(1/\mu)$ in Eq. (1), we obtain

$$B = \frac{2\phi_0}{\sqrt{3}\lambda^2}\left[\ln\left[\frac{3\phi_0}{4\pi\mu\lambda^2(H - H_{c1})}\right]\right]^{-2}, \quad H \approx H_{c1} \quad (2)$$

for H just greater than H_{c1}, and

$$B \approx \mu\left[H - H_{c1}\frac{\ln(H_{c2}/B)}{\ln(\kappa)}\right], \quad (H_{c1} \ll H \ll H_{c2}) \quad (3)$$

at intermediate fields. Apart from the slowly varying logarithmic term, we find that B increases by a factor of μ for both low $H \approx H_{c1}$ and intermediate H, therefore, probably for all H,

$$B(\chi) = \mu B(\chi = 0) \,. \quad (4)$$

The factor μ is traced to the factor $(1/\mu)$ in Eq. (1). It is clear that the reduction in the penetration depth is mainly responsible for the increase in B. The equilibrium magnetization is

$$4\pi M = B - H = \mu(4\pi M_{\chi=0}) + 4\pi\chi H \quad (5)$$

with $4\pi M_{\chi=0} = B(\chi = 0) - H$. $4\pi H$ is roughly sketched in the inset of Fig. 1. At low H, the effect of χ on the magnetization is small and difficult to observe experimentally because of the large Meissner signal and flux pinning. Therefore, of more interest is the flux density at the intermediate H regime, at which the magnetic ion contribution is comparable to, or greater than, that of the Meissner effect.

III. FLUX MOTION AND CRITICAL-STATE MODEL

Using $H_{c2} \gg B \approx \mu H$, we rewrite Eq. (3) as

$$B = (1+4\pi\chi)H - H_r \,. \quad (6)$$

The diamagnetic term is replaced by H_r, which is essentially the reversible diamagnetism at any given H associated with the Meissner effect. H_r may have a similar T dependence as H_{c1}. Equation (4) shows that the magnetic ions contribute to the total magnetization in the form of flux lines. In this sense, χ in Eq. (6) is rather a measure of the additional vortices than a measure of the induced moment. The actual flux motion depends on the variation of

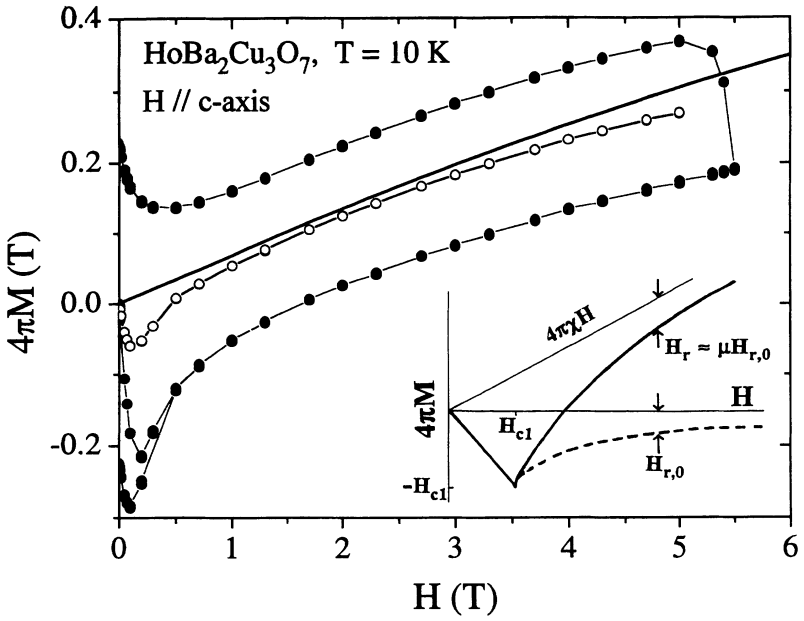

FIG. 1. Magnetic isotherm $M(H)$ at 10 K (solid circles) and its average M_{avg} (open circles). The thick solid line is the calculated magnetic moment of the Ho^{3+} ions (Ref. 2). The enhancement of Meissner diamagnetism is invisible since μ is close to 1. The inset sketches $M(H)$ from Eq. (5). It is similar to M_{avg} except the CFE region.

$B(H,T)$. In a magnetic isotherm no anomaly due to the magnetic medium arises, but the medium slightly modifies the $M(H)$ curve. The enhancement of diamagnetism in Eq. (5) may be invisible because μ is close to 1. In flux expulsion, flux motion changes at T_M, at which $\partial B/\partial T=0$. When a specimen is cooled through the superconducting transition temperature T_c in an intermediate H, flux lines move out because $H_r \sim H_{c1} \sim (1-t^2)$ varies faster than $4\pi\chi H \sim t^{-1}$, where $t \equiv T/T_c$, unless H is too large. Below T_M, where $\partial B/\partial T>0$, flux lines move into the specimen through the surface. When the specimen temperature increases, flux lines move out below T_M, and move in above it. Flux pinning hinders this flux motion, resulting in a greater M_{FCW} than M_{FCC}, where M_{FCC} and M_{FCW} are field-cooled (FC) magnetization measured with decreasing T (FCC) and increasing T (FCW), respectively. The flux profile under flux pinning is given by the solution of the critical-state relation $\nabla \times \mathbf{B}=(4\pi/c)\mathbf{J}_c$, for instance, in cylindrical coordinates, where J_c is the critical current density.[6] In this case, B in Eq. (6) serves as the flux density at the surface:

$$B(r)=[1+4\pi\chi(t,H)]H-H_r(t,H) \pm \left[\frac{4\pi}{c}\right]J_c(t,H)(r-R) . \quad (7)$$

H is assumed to be parallel to a cylindrical sample with radius R. The + (or −) sign preceding the J_c term is for a flux moving-in (or moving-out). The magnetization with flux pinning is $4\pi M=\langle B-H\rangle$, where $\langle\ \rangle$ denotes the average over the area normal to H.

IV. EXPERIMENTAL, RESULTS, AND DISCUSSION

The sample used in this experiment was HBCO powder with grain sizes of between 45 and 63 μm. The powder was mixed with vacuum grease and grain aligned in a commercial superconducting quantum interference device magnetometer (Quantum Design, Inc.). Both $M(T)$ and $M(H)$ data were taken for fields parallel to the c axis of the specimen in the same data acquisition conditions as in Ref. 8. Possible measurement artifacts due to size effects, ferromagnetic impurities, or flux creep were carefully examined. $M(T)$ data at $H=1$ T between 100 and 300 K best fit the Curie-Weiss (CW) relation, $4\pi\chi(T)\equiv 4\pi M/H=4\pi\chi_0+C/(T+\Theta)$ with $4\pi\chi_0=1.3\times10^{-4}$, $C=1.67$ K, and $\Theta=14.5$ K. The calculated effective moment of the specimen was $10.5\pm0.2\mu_B$ per formula unit, equal to that of a free Ho^{3+} ion. Figure 1 illustrates the magnetic isotherm at 10 K (solid circles). The open circles show the average of $M(H)$, $M_{avg}=\frac{1}{2}[M(H\text{-increase})+M(H\text{-decrease})]$. The solid line, calculated by Eq. (3) in Ref. 2, is the magnetic moment due to the Ho^{3+} ions with a saturation moment of $10.6\mu_B$ ($g_J=1.25$ and $J=8$) and T shifted by Θ. This line runs approximately parallel to M_{avg}, in the middle of the hysteresis loop. This difference between the solid line and M_{avg} at 1 T was 146 G, roughly the value of H_r. The difference becomes greater at higher fields, probably indicative of strong CFE. However, the electromagnetic interaction between superconductivity and local moments is not easily seen in the magnetic isotherm because $M(H)$ of HBCO is similar to {Ho^{3+} moment $+M(H)$ of YBCO} except CFE. On the other hand, the interaction is clearly demonstrated in the flux expulsion. Figure 2(a) exhibits $M(T)$ data at $H=1$ T (open circles), showing $F_{FCW}>M_{FCC}>0$ except near T_c. The hysteresis $\Delta(4\pi M)=4\pi(M_{FCW}-M_{FCC})$ becomes greater the higher the H and the lower the T_L, the lowest measuring temperature. The maximum $\Delta(4\pi M)$ was 20 G for $H=1$ T, but 150 G for $H=5$ T at around 30 K when $T_L=10$ K. It is obvious that this hysteresis is not obtained by adding $4\pi\chi H$ to $M(T)$ of YBCO. For the $M(T)$ calculation, we

employed $H_r(t)=H_r(0)(1-t^2)$, $J_c(t)=J_c(0)(1-t)^n$, and $\gamma=(4\pi/c)RJ_c(0)/H_r(0)$, which were useful for YBCO.[8] In addition, aside from its validity, we used the above $\chi(t)$, which was measured above T_c and extrapolated to temperatures down to $T_L=10$ K. The solid line in Fig. 2(a) is the model fit for $H=1$ T using Eq. (7), with the parameters $H_r(0)=125$ G, $\gamma=25$, and $n=6$. Figure 2(b) shows the flux profiles for the FCC process in the model fit. Two flux freezing profiles are shown by the curve *TM*, which looks like a straight line, for the flux move-out, and by the curve *C* below 56 K for the flux move-in.

When the specimen temperature increases from T_L in the FCW process, the flux lines not only move out from the surface of the specimen, but also move into the center region of the specimen, at which B is low. This flux motion leaves a Λ-shaped maximum, which is equivalent to the V-shaped minimum for the YBCO case.[6] Based on the above idea, the flux profile $B(r)$ at 36 K for the FCW process is schematically sketched by the broken line F in Fig. 2(b), showing a Λ-shaped maximum in $B(r)$. From the $B(r)$ for FCC and FCW processes, we see that M_{FCC} is smaller than M_{FCW}, qualitatively explaining the hysteretic $M(T)$ data. The FCW magnetization was not calculated because the position of the maximum remained to be estimated. This Λ-shaped maximum also qualitatively accounts for the T_L dependence of zero-field-cooled (ZFC) magnetization M_{ZFC} at intermediate H. Flux lines in the ZFC process move out of the specimen from the edge and partially move into the core region as T increases from T_L, at which H is turned on. Therefore, at $T=T_1$ ($>T_L$), the flux profile, for which H is turned on at $T=T_L$, can be different from that for which H is turned on at $T=T_1$.[20]

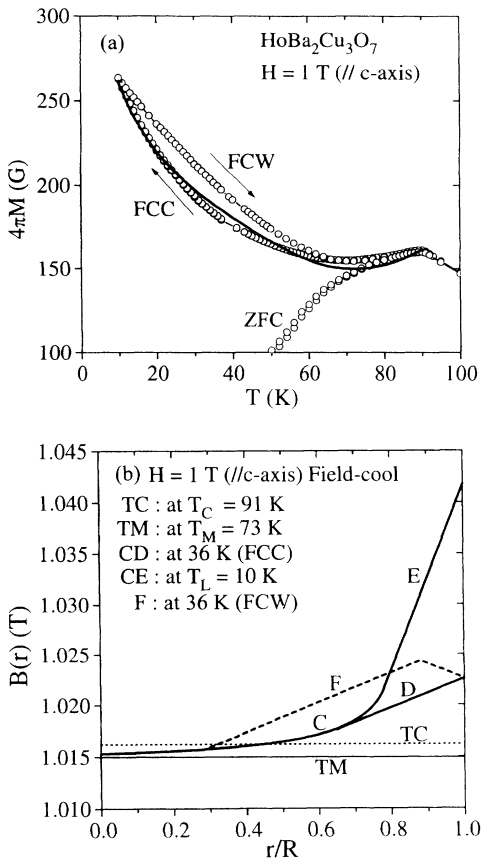

FIG. 2. (a) Flux expulsion $M(T)$ for HBCO at $H=1$ T parallel to the c axis, showing $M_{FCW}>M_{FCC}>0$. The solid line is the model fit for the FCC data. (b) Flux profiles $B(r)$ for the FCC process in (a) are exhibited by *TC* (thin dotted line) at $T_c=91$ K, by *TM* (thin solid line) at $T_M=73$ K, by *CD* at 36 K, and by *CE* at $T_L=10$ K. The curve $B(r)$ is due to flux freezing. The broken line F is a sketch for the flux profile at 36 K in the FCW process. The line F is not numerically correct but is to show qualitatively the Λ-shaped maximum in $B(r)$. Numerical prediction of M_{FCW} was not made because the position for the Λ-shaped maximum remains to be estimated. At higher fields, for instance, $H=5$ T, the segment *CE* moves toward the center, causing greater hysteresis.

The model fit in Fig. 2 was made using the FCC data. In this model fit, we used the same T dependence of $H_r(t)$ and $J_c(t)$ for HBCO as those for YBCO. Whereas $H_r(t)$ and $J_c(t)$ are parameters in the model fit, $\chi(t)$ is not a parameter, but a quantity to be determined by a separate $\chi(t)$ measurement. We used the $\chi(t)$ obtained by measuring $M(t)$ for 100 K $<T<$ 300 K and extrapolating it down to $T_L=10$ K. Care has to be taken for the extrapolation. The actual $\chi(t)$ for HBCO approximately follows the CW relation down to about 10 K, but significantly deviates from it at temperatures lower than 5 K, as determined by the neutron-scattering experiment.[5] For instance, $\chi(t)$ along the c axis decreases as T decreases below 10 K. In addition, whereas the magnetic easy axis is parallel to the c axis above 100 K, χ along the a axis is much greater than that along the c axis at low temperatures. Therefore, the apparent χ in the c axis may be effectively greater than the true value since a vortex due to H parallel to the c axis may have the *ab* component by the vortex wiggling and tangling. For this reason, $ErBa_2Cu_3O_7$, which has greater χ along the c axis at low temperatures,[21] may be more suitable to demonstrate the model.

There were three functions to be determined in the model calculation, $\chi(t)$, $H_r(t)$, and $J_c(t)$, and no unique set of the functions giving a precise fit for the data was found. Even so, the model prediction of hysteresis in $M(t)$ clearly demonstrated flux quantization and magnetic ion contribution by superconducting vortices as stated above. Although this is analogous to flux quantization in the paramagnetic state above the Curie temperature of a ferromagnetic superconductor, it has been ignored in the magnetization measurement of cuprate superconductors with paramagnetic ions such as RBCO. The current experiment suggests that the interaction between local moment and superconductivity should be considered in the magnetization measurements for magnetic superconductors, even those with small susceptibility. Also of interest is the experimental detection of a reduction in λ due to the magnetic ions. It may be possible to observe this λ reduction due to the large susceptibility at low temperatures in the a axis of an untwinned HBCO single crystal[5] or in the c axis of $ErBa_2Cu_3O_7$.[21] This λ reduction, which

is independent of the origin of superconductivity, must occur with any induced magnetic moment. It might be worth considering whether this produces nontrivial changes which might cause inconsistency in $\lambda(T)$ measurements at low temperatures.[22]

V. SUMMARY

In summary, based on the London model, it was shown that the induced local moments in a paramagnetic superconductor such as RBCO reduce the penetration depth by a factor of $\mu^{-1/2}$, and increase the equilibrium flux density by a factor of μ. The λ reduction plays the crucial role in increasing B. As a result, the specimen introduces additional vortices associated with the medium, which are subject to anisotropy and flux pinning. Thus, the magnetic ions in a type-II superconductor contribute to the magnetization in the form of a superconducting vortex. The hysteretic flux expulsion of HBCO at intermediate fields was explained using the critical-state model together with the above analysis. In the flux expulsion for intermediate fields ($H_{c1} \ll H \ll H_{c2}$), at which the induced moment is greater than the Meissner diamagnetism, vortices move into the specimen as temperature decreases, causing greater flux density near the surface than in the core region. When temperature increases, the vortex structure relaxes so that vortices move toward the lower B region; i.e., partially move out from the specimen and partially move into the center region, leaving a Λ-shaped maximum. This flux motion results in different $M(T)$ patterns with hysteresis from those for YBCO.

ACKNOWLEDGMENT

The authors are grateful to S. Maekawa for discussions about the early work on ferromagnetic superconductors.

[1]L. F. Schneemeyer, J. V. Waszczak, S. M. Zahorak, R. B. van Dover, and T. Seigrist, Mater. Res. Bull. **22**, 1467 (1987).

[2]J. R. Thompson, D. K. Christen, S. T. Sekula, B. C. Sales, and L. A. Boatner, Phys. Rev. B **36**, 836 (1987).

[3]M. Wacenovsky, H. W. Weber, O. B. Hyun, D. K. Finnemore, and K. Mereiter, Physica C **160**, 55 (1989).

[4]L. W. Roeland, F. R. de Boer, Y. K. Huang, A. A. Menovsky, and K. Kadowaki, Physica C **152**, 72 (1988); F. Zuo, B. R. Patton, D. L. Cox, S. I. Lee, Y. Song, J. P. Golben, X. D. Chen, S. Y. Lee, Y. Cao, Y. Lu, J. R. Gaines, J. C. Garland, and A. J. Epstein, Phys. Rev. B **36**, 3603 (1987).

[5]A. Furrer, P. Brüesch, and P. Unternährer, Phys. Rev. B **38**, 4616 (1988).

[6]J. R. Clem and Z. Hao, Phys. Rev. B **48**, 13 774 (1993).

[7]O. B. Hyun, Phys. Rev. B **48**, 1244 (1993); J. Deak, M. McElfresh, J. R. Clem, Z. D. Hao, M. Konczykowski, R. Muenchausen, S. Foltyn, and R. Dye, Phys. Rev. B **49**, 6270 (1994).

[8]O. B. Hyun, Physica C **206**, 169 (1993).

[9]C. P. Bean, Phys. Rev. Lett. **8**, 250 (1962); Rev. Mod. Phys. **36**, 33 (1964).

[10]Ming Xu, in *Studies of High Temperature Superconductors,* edited by A. Narlikar (Nova Science, New York, 1993), Vol. 11, p. 79.

[11]L. Krusin-Elbaum, A. P. Malozemoff, D. C. Cronemeyer, F. Holtzberg, J. R. Clem, and Z. Hao, J. Appl. Phys. **67**, 4670 (1990).

[12]T. Matsushita, E. S. Otabe, T. Matsuno, M. Murakami, and K. Kitazawa, Physica C **170**, 375 (1990); K. Kitazawa, Y. Tomioka, T. Hasegawa, K. Kishio, M. Naito, T. Matsushita, I. Tanaka, and H. Kojima, Supercond. Sci. Technol. **4**, S35 (1991).

[13]S. Maekawa, M. Takahashi, and S. Tachiki, J. Magn. Magn. Mater. **13**, 324 (1979); A. Kotani, M. Tachiki, H. Matsumoto, H. Umezawa, and S. Takahashi, Phys. Rev. B **23**, 5960 (1981).

[14]H. Umezawa, H. Matsumoto, and J. P. Whitehead, in *Superconductivity in Magnetic and Exotic Materials,* edited by T. Matsubara and A. Kotani (Springer-Verlag, Berlin, 1984), p. 29.

[15]H. R. Ott, H. Rudiger, H. C. Hamaker, and M. B. Maple, in *Ternary Superconductors,* edited by G. K. Shenoy, B. D. Dunlap, and F. Y. Fradin (North-Holland, Amsterdam, 1981), p. 159; K. P. Sinha and S. L. Kakani, *Magnetic Superconductors* (Nova Science, New York, 1989).

[16]T. Koyama, S. Maekawa, and M. Tachiki, J. Phys. Soc. Jpn. **52**, 1750 (1983); M. Tachiki, H. Matsumoto, T. Koyama, and H. Umezawa, Solid State Commun. **34**, 19 (1980).

[17]P. Fischer, K. Kakurai, M. Steiner, K. N. Clausen, B. Lebech, F. Hulliger, H. R. Ott, P. Brüesch, and P. Unternährer, Physica C **152**, 145 (1988).

[18]Low dimensionality of the vortex structure was not considered here. The characteristic lengths λ and ξ must be λ_{ab} and ξ_{ab}, respectively, for H parallel to the c axis, where ab denotes the conducting Cu-O plane of HBCO.

[19]M. Tinkham, *Introduction to Superconductivity* (McGraw-Hill, New York, 1975), p. 144.

[20]O. B. Hyun and I. Hirabayashi, in *Advances in Superconductivity-VI,* edited by T. Fujita and Y. Shiohara (Springer-Verlag, Tokyo, 1994), p. 577.

[21]L. Soderholm, C.-K. Loong, and S. Kern, Phys. Rev. B **45**, 10 062 (1992).

[22]Z. Ma, R. C. Taber, L. W. Lombardo, A. Kapitulnik, M. Beasley, P. Merchant, C. B. Eom, S. Y. Hou, and J. M. Phillips, Phys. Rev. Lett. **71**, 781 (1993), and references therein.